33rd Annual International Conference of the IEEE EMBS
Boston, Massachusetts USA, August 30 - September 3, 2011

Comparison between EEMD, Wavelet and FIR Denoising: Influence on Event Detection in Impedance Cardiography

S. De Ridder, X. Neyt, *Member, IEEE*, N. Pattyn and P-F. Migeotte

***Abstract*— During thoracic impedance signal acquisition, noise is inherently introduced and hence, denoising is required to allow for accurate event detection. This paper investigates the effectiveness of Ensemble Emperical Mode Decomposition to filter random noise. The performance of the EEMD method is compared with an optimal FIR filter and wavelet denoising. The IMF selection for signal reconstruction in the EEMD denoising method is optimized using a sequential search. Denoising performance was evaluated by the SNR and the accuracy in event detection after filtering. When all criteria are taken into account, wavelet seems to outperform both EEMD and FIR denoising.**

I. INTRODUCTION

Impedance cardiography (ICG) has been extensively studied as a non-invasive and cost-effective method for monitoring cardiac function. Electrodes placed on the thorax measure changes in electrical impedance, Z, caused by the fluctuating blood volume during each cardiac cycle [1]. Figure 1 shows part of an ECG (R-R interval) signal and the corresponding negative time derivative of the electrical impedance ($-dZ/dt$) signal, the ICG signal. Various points related to events in the cardiac cycle can be detected on the $-dZ/dt$ curve. The B point is associated with aortic valve opening, while the X point corresponds to the aortic valve closure. The difference in time between these two points corresponds to the Left Ventricular Ejection Time (LVET) and is used, together with the maximum change in impedance $(-dZ/dt)_{max}$, to calculate the (beat-by-beat) Stroke Volume (SV) using e.g. the Kubicek formula [1]:

$$SV = \rho_b (L/Z0)^2 LVET \, (-dZ/dt)_{max} \qquad (1)$$

where ρ_b is the resistivity of blood, L is the distance between the recordings electrodes and Z_0 is the baseline impedance between the recording electrodes. The problem is therefore to accurately detect the B, X and C points from the $-dZ/dt$ signal. However, during the impedance signal acquisition, noise is inherently introduced and hence, denoising is required to detect the physiological events as accurately as possible.

In ICG signal signal acquisition, noise can be of various origin: electronic noise, motion and respiration artifacts, electromyographic interference, etc... In this paper, only random noise is considered. Ensemble Empirical Mode Decomposition (EEMD) is a novel recently developed algorithm for the analysis of non-stationary signals [2] and has the potential to filter electronic noise from the ICG signal. The purpose of this paper is to investigate the performance of EEMD in removing electronic noise from the ICG signal and to study the influence of EEMD denoising on the detection of the B, C and X points. The performance of the EEMD method is compared with an optimal FIR filter and wavelet denoising.

Manuscript received April 15, 2011. This research is supported by the Belgian Federal Science Policy Office (BELSPO) via the European Space Agency PRODEX program.

S. De Ridder, X. Neyt, N. Pattyn and P-F. Migeotte are with the Signal and Image Centre of the Royal Military Academy, 1000, Brussels, Belgium (email: sven.de.ridder@elec.rma.ac.be)

II. METHOD

A. Reference Signal

An ICG signal obtained with the Russian Pneumocard device was used to create a reference signal. The measured signal was bandpass filtered (0.5 - 30 Hz) and sampled with a sampling rate of 1 kHz. From the resulting ICG signal, four ICG cycles (four R-R intervals in the ECG signal) were selected to form the master signal. These four cycles were chosen during a breathhold period, which assures that no respiration artifacts are included in the signal. Also, the subject was not moving during the measurement and hence, no motion artifacts are present. The master signal consists of four cycles to include a natural diversity in the ICG signal. Fig. 1 shows the master ICG signal and the corresponding ECG. The reference ICG signal was then created by amending copies of the master ICG signal and truncating the resulting signal to a dyadic length, resulting in a final reference signal with a duration of 32 seconds. The mean $LVET$ and $(-dZ/dt)_{max}$ of the reference signal are 0.21 seconds and 5.10 Ω, respectively.

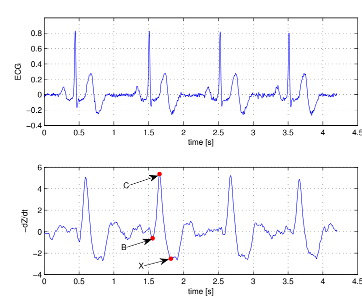

Fig. 1. Master $-dZ/dt$ signal and corresponding ECG

B. Noise Simulation and Performance Criteria

White Gaussian noise is added to the reference signal to simulate electronic noise. Different input noise levels were tested (0, 5, 10, 15 and 20 dB). The procedure, i.e., adding noise and filtering, is repeated 50 times per noise level. After denoising, the signal-to-noise ratio is calculated using:

$$SNR_{out} = 20\, log_{10}(\frac{||x_{ref}||}{||x_{ref} - x_{filt}||}) \tag{2}$$

where x_{ref} is the clean reference signal and x_{filt} is the filtered signal. $LVET$ and $(-dZ/dt)_{max}$ are calculated from the timing of the B and X event and the amplitudes of the B and C events, respectively. Therefore, the influence of denoising on these four parameters are calculated as Δ = $event_{ref}$ - $event_{filt}$. A positive Δ yields a timing shift to the left (earlier detection) or a downward amplitude shift (lower amplitude). The overall performance of one denoising method, per input noise level, is analyzed by calculating the mean and standard deviation of the SNR and four Δs over all the 50 realizations. The higher the SNR and the lower the Δ, the better the performance.

C. Event Detection

First, the instant of the $(-dZ/dt)_{max}$ (point C) is determined on the ICG tracing delimited by two successive R peaks. Then, starting from this point and descending backward on the ICG curve, the B point is determined as the point where the second derivative of the ICG curve is maximum. Finally, going forward from the $(-dZ/dt)_{max}$ point, the closing event (point X) is determined as the point where the second derivative of the ICG curve is maximum, with the condition that this point is below 10% of the $(-dZ/dt)_{max}$ threshold.

D. EEMD-based Denoising

Empirical Mode Decomposition (EMD), introduced by Huang et al. [3] adaptively decomposes a signal $x(t)$ into N Intrinsic Mode Functions $c_j(t)$. EMD separates the full signal into ordered elements with frequencies ranged from higher to lower frequencies in each IMF level [4]. After EMD, the signal is given as:

$$x(t) = \sum_{j=1}^{N} c_j(t) + r(t) \tag{3}$$

where $r(t)$ is the residue after N IMFs have been extracted and can be considered as $c_{N+1}(t)$. The IMFs represent zero-mean AM/FM components [3], while the residue is a non-zero mean low order polynomial [2]. The EMD algorithm consists of the following steps [3]:

- Identify all the maxima and minima extrema of the signal $x(t)$.
- Generate the upper and lower envelope by interpolation between the minima and maxima extrema, respectively.
- Calculate the mean function of the upper and lower envelope: $m(t)$.
- Compute the difference signal $d(t) = x(t) - m(t)$.
- Replace $x(t)$ with $d(t)$ and iterate the previous four steps until $d(t)$ becomes zero-mean. Then, $d(t)$ is IMF 1 and is named $c_1(t)$.
- Calculate the residue signal $r(t) = x(t) - c_1(t)$ and repeat the procedure as specified by all previous step with $x(t)$ replaced by $r(t)$ to obtain IMF 2. To obtain all IMFs, repeat all the steps N times until the final residual signal is a monotonic function.

The major disadvantage of EMD is the mode mixing effect, which indicates that oscillations of different time scales coexist in a given IMF, or that oscillations with the same time scale have been assigned to different IMFs [4]. This mode mixing effect could make the physical meaning of an individual IMF unclear. Therefore, Ensemble EMD (EEMD) was introduced to remove the mode-mixing effect [2]. Using EEMD, white noise is added to the signal in many realizations. The noise in each realization is different and the added noise can be canceled out on average, if the number of trials is sufficient [4]. In every trial, the signal (contaminated by white noise) is decomposed into IMFs as described previously. Then, the obtained IMFs are ensemble averaged to arrive at the final result. In the current paper, the values as suggested by Wu and Huang in [2] are used: white noise of amplitude 0.2 times the standard deviation of $x(t)$ and 100 realizations.

Denoising a signal using EEMD consists in partially reconstructing the signal using Eq. 3, by only using some specific useful IMFs. In the current paper, a similar approach as in [4] is used, where both high level and low level IMFs are eliminated, resulting in a band-pass type filter.

E. Optimal FIR filter

The frequency response of a FIR filter depends on its coefficients, which in turn are related to the desired cut-off frequency (f_c) and the order of the filter (n). To compare the performance of EEMD with the best possible solution using a FIR filter, a Genetic Algorithm (GA) is used to find the optimal vales of f_c and n. The GA searches for the combination of f_c and n resulting in the largest SNR after filtering. Figure 2 shows the frequency responses of the obtained optimal FIR filters, on top of the PSD of the $-dZ/dt$ signal [5]. The corresponding f_c and n values are also indicated. Forward and reverse filtering is used to eliminated phase distortion.

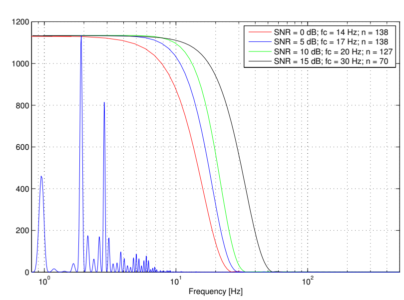

Fig. 2. PSD of $-dZ/dt$ and frequency responses of optimal FIR filters

F. Wavelet-based filtering

During Wavelet analysis, the inner product is taken of the input signal $x(t)$ and some basis functions. The similarity between the signal and basis functions is measured and coefficients indicate how close the signal is to the basis function. All basis functions are scaled versions of the same prototype or mother wavelet. Denoising using wavelet decomposition is performed by selecting the coefficients that will be used for the reconstruction of the filtered signal.

The Matlab toolbox Wavelab 850 was used for wavelet denoising. The Symmlet 8 is chosen as the mother wavelet. Coefficient selection is done by hard thresholding, using the thresholds determined with the SURE method and increased with a factor 2 to eliminate some noise components otherwise present [5].

III. RESULTS AND DISCUSSION

A. Signal-to-noise ratio after filtering

Figure 3 shows the SNR values after denoising using the optimal FIR filter, Wavelet and EEMD with optimal IMF selection. Both the mean and the standard deviation of the 50 repetitions are presented as a function of the input noise level. All denoising methods result in an increase of SNR after filtering. EEMD provides higher SNR values than Wavelet-based filtering. However, the optimal FIR filter outperforms both EEMD and Wavelet denoising. EEMD is much more computationally intensive (factor 1000) than Wavelet denoising.

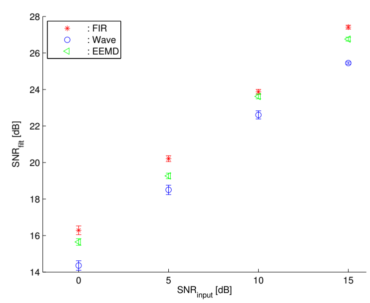

Fig. 3. SNR after denoising as a function of the input noise level.

The optimal IMFs used in EEMD denoising are found by a sequential search. This approach is similar as in [4] and the cost function to be optimized is the SNR after filtering. As an example, consider Fig. 4, which shows the contour map of SNR values after EEMD denoising as a function of the selected IMFs for a noisy ICG (5dB). No SNR values are given for the lower right part, since the initial IMF must be smaller than the final one. The red dot indicates the optimal IMF combination. Reconstructing the filtered signal using IMF 6 till IMF 12 and including the residual results in the maximum SNR after filtering. The low IMF scales contain high frequency components of the signal, while the high IMF scales correspond to the low frequency components of the signal. Hence, using IMF 6 till IMF 12 corresponds to a bandpass filter.

The sequential search procedure is repeated for every input noise level, resulting in changing IMF boundaries for different noise levels, see Table I. The higher the input noise level, the less IMFs are used for signal reconstruction. A

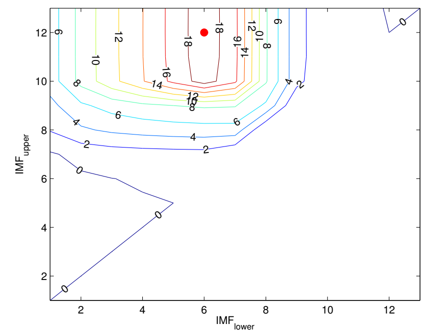

Fig. 4. Contour map of SNR as function of selected IMFs; RED dot: optimal IMF boundaries

trade-off is performed between eliminating noise and using more IMFs to capture details of the signal.

TABLE I
OPTIMAL IMF SELECTION FOR MAXIMAL SNR

SNR_{in}	$IMF1$	$IMF2$
0dB	7	11
5dB	6	12
10dB	6	13
15dB	5	13

B. Influence of filtering on the B, C and X point

In ICG analysis, rather than obtaining the best SNR, it is more important to accurately detect events from which the $LVET$ and $(-dZ/dt)_{max}$ can be deduced.

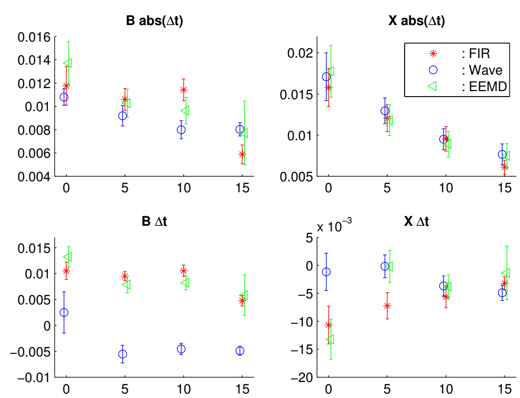

Fig. 5. Mean absolute error and mean error of B and X event timings. X-axis: SNR_{input} [dB]; Y-axis: Δt [s]

Figure 5 presents the changes in timing of the B and X events due to denoising. Both the mean absolute error and mean error are given, together with the standard deviation. The absolute error in timings decreases for lower input noise levels. For the B timing, wavelet denoising results in the lowest absolute error (except for low input noise of 15dB SNR). The absolute error in X timing is in general higher than the error in B timing, but no clear advantage for one of the three methods can be identified. Comparing the absolute error with the mean error for the B timing indicates that for EEMD and the optimal FIR filter these two values are close together, meaning that both denoising algorithms introduce a systematic shift to the left (earlier detection of B event). After wavelet denoising, the B point is shifted to the right (later detection), except at high input noise levels, but a lower shift is introduced with respect to the other two methods. For the X event timing, all methods introduce a shift to the right (later detection of X event). Only a small shift is introduced after wavelet denoising, even at high input noise levels. Table II presents the % change in mean LVET due to a combined error in B and X timings. Wavelet introduces the least amount of change in LVET (error lower than 3%), because it has the lowest mean change in both B and X timings and shifts both points in the same direction (later detection). Except for a high input noise level, EEMD performs better than the optimal FIR filter. However, the changes for both methods in LVET are much larger because the B point is detected earlier while the X point is detected later and hence, the LVET is increased (error up to 13%).

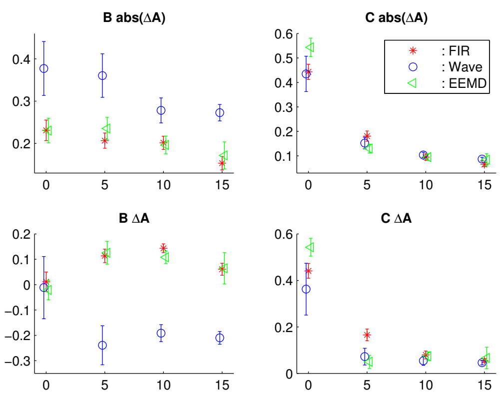

Fig. 6. Mean absolute error and mean error of B and C event amplitudes. X-axis: SNR_{input} [dB]; Y-axis: Δ amplitude [Ω]

Figure 6 shows the mean absolute error and mean error of the B and C event amplitudes due to denoising. The absolute error in the amplitude of the B event is the largest after the wavelet denoising. EEMD and FIR yield similar absolute errors in B amplitude. The mean error in B amplitude show that the B event after wavelet denoising is shifted upward (larger amplitude), while the B event is shifted downward after optimal FIR and EEMD filtering. Regarding the absolute error in the C amplitude, the three denoising methods have comparable performances. The biggest error in the amplitude occurs at a high input noise level after EEMD denoising. Wavelet yields the largest standard deviation. All three denoising methods introduce a systematic downward shift of the C event. Table II presents the % change in mean $(-dZ/dt)_{max}$ due to a combined error in B and C amplitudes. In case of an input noise of 0 dB SNR, the wavelet denoising methods yields the lowest change, with an error of -7% (underestimation). However, at lower input noise level, the performance of wavelet denoising is considerably lower than the other two methods. Wavelet denoising introduces an upward shift of the B event and downward shift of the C event, yielding large underestimations of $(-dZ/dt)_{max}$. The optimal FIR filter and EEMD introduce a downward shift of both the B and C amplitude, resulting in lower errors of $(-dZ/dt)_{max}$. A possible cause for the high errors in event amplitude after wavelet denoising is the coefficient selection. The thresholds obtained by the SURE method were multiplied by a factor 2, for all input noise levels. Although higher thresholds are required at high input noise levels, lower thresholds at lower input noise levels might decrease the amplitude errors. Further research is required to optimize the thresholds.

TABLE II
% CHANGE IN LVET AND $(-dZ/dt)_{max}$

	SNR_{in}	FIR	Wavelet	EEMD
$LVET$	0dB	10.3	**1.8**	12.8
	5dB	8.1	**-2.6**	3.9
	10dB	7.9	**-0.4**	5.8
	15dB	3.9	**0.0**	3.5
$(-dZ/dt)_{max}$	0dB	-8.4	**-7.3**	-11.1
	5dB	**-1.0**	-6.1	1.5
	10dB	1.3	-4.8	**0.7**
	15dB	0.1	-5.0	**-0.1**

IV. CONCLUSIONS

EEMD yields higher SNRs after filtering than wavelet denoising, but the optimal FIR filter results in the highest SNRs. Optimal IMF selection shows that the higher the input noise level, the less IMFs are used for signal reconstruction. Wavelet denoising introduces the least amount of change in B and X event timings (LVET error of maximum 3%), while EEMD and the optimal FIR filter introduces significant larger errors. However, wavelet introduces large error in B and C event amplitude, leading to errors in $(-dZ/dt)_{max}$ of up to 7%, while EEMD and FIR yield lower errors. If it is possible to decrease the amplitude errors by optimizing the thresholds and taken into account the low computation time, the low distortion of event timings and low errors in $LVET$, the results suggest that wavelet-based filtering is the best option to denoise an ICG signal with the least amount of event distortion.

REFERENCES

[1] W. G. Kubicek et al., "Development and evaluation of an impedance caridac output system", Aerospace Medicine 39:248-252; 1966.
[2] Wu, Z., Huang, N.E., "Ensemble Empirical Mode Decomposition: a Noise-Assisted Data Analysis Method", Advances in Adaptive Data Analysis, vol. 1, no. 1, pp. 1-41.
[3] Huang, N.E., Shen, Z., Long, S.R., Wu, M.C., Shih, H.H., Zheng, Q., Yen, N.C., Tung, C.C., Liu, H.H., "The empirical mode decomposition and the Hilbert spectrum for nonlinear and non-stationary time series analysis", Proc. Roy. Soc. Lond. 1998, 454, 903-995.
[4] Chang, K-M., " Arrhythmia ECG Noise Reduction by Ensemble Empirical Mode Decomposition", Sensors 2010, 10, 6063-6080.
[5] De Ridder, S., Peeters, T., Pattyn, N., Neyt, X., Migeotte, P-F., "EEMD Denoising of Thoracic Impedance Cardiogrpahy", Proc. WIC/IEEE SP Symposium on Information Theory and Signal Processing in the Benelux, Brussels, May 2011